**Oral Diseases (2009) 15**, 273–280. doi:10.1111/j.1601-0825.2009.01522.x

http://www.blackwellmunksgaard.com

ORIGINAL ARTICLE

# Micro-CT analysis of alveolar bone healing using a rat experimental model of critical-size defects

**H Ebina[1,2], J Hatakeyama[3], M Onodera[4], T Honma[2,5], S Kamakura[6], H Shimauchi[1], Y Sasano[2]**

*Divisions of [1]Periodontology and Endodontology, [2]Craniofacial Development and Regeneration, Tohoku University Graduate School of Dentistry, Sendai; [3]Functional Structure Section, Department of Morphological Biology, Fukuoka Dental College, Fukuoka; [4]First Department of Oral Anatomy, School of Dentistry, Iwate Medical University, Morioka; [5]Oral Surgery, Tohoku University Graduate School of Dentistry, Sendai; [6]Bone Regenerative Engineering Laboratory, Graduate School of Biomedical Engineering, Tohoku University, Sendai, Japan*

**OBJECTIVE: This study was designed to establish a rat model of a critical size alveolar bone defect.**

**MATERIALS AND METHODS: Standardized buccal or mesiobuccal alveolar bone defects were made around the right first mandibular molar of 12-week-old rats, and the left was used as a control. Alveolar bone healing was examined quantitatively by three-dimensional micro-computed tomographic imaging. Bone matrix production of osteoblasts and osteocytes during repair of alveolar bone defects was examined with *in situ* hybridization for type I collagen.**

**RESULTS: Buccal defects were repaired significantly and the volume decreased by 88.3% in week 24, whereas mesiobuccal defects were repaired little. Osteoblasts and osteocytes expressed type I collagen in both defects in week 3 but showed little expression by week 6 and thereafter, leaving the mesiobuccal defects largely unrepaired.**

**CONCLUSION: The mesiobuccal defect is a critical-size defect that is not ultimately repaired with bone. It may be an appropriate experimental model for investigating the effectiveness of bone regenerative agents in human alveolar bone loss.**

*Oral Diseases* (2009) **15**, 273–280

**Keywords:** alveolar bone; defect; repair; rats; micro-CT

## Introduction

A number of animal models have been used to study effectiveness of regenerative agents in alveolar bone loss. Primates are considered suitable because the morphological features of their teeth and periodontal tissues closely resemble those of humans (Fritz *et al*, 2000). Dogs are used frequently, owing to their accessible size of their teeth and ease of handling (Wikesjö *et al*, 2003). However, the low cost, short study intervals, small variation among strains and known genetics make murine models extremely attractive in the study of alveolar bone loss (Wilensky *et al*, 2005). Rats have the advantage over mice because of the size and the accessibility of their teeth and periodontal tissues, and therefore have potential as the ideal animal model of alveolar bone loss.

It has been suggested that the repair of bone defects depends on the size of the defect; that is, a bone defect larger than a certain size (a critical size) cannot be healed with bone. The remaining defect is filled with fibrous connective tissues (Honma *et al*, 2008). Calvarial critical-size bone defects have been used in various studies to investigate the effectiveness in bone defect repair of bone regenerative agents such as growth factors, biomaterials, cell or tissue implantation, or any combination of these (Kamakura *et al*, 1999, 2004, 2006; Lutolf *et al*, 2003; Cowan *et al*, 2004, 2005). The critical-size defect model would also benefit research on repair of alveolar bone loss, but no feasible animal model of the critical-size defect has been developed for alveolar bone loss. This study was designed to establish a model for critical size defects of alveolar bone in rats, which could mirror alveolar bone loss in humans. We aimed to capture the process of alveolar bone healing in large defects compared with that in small defects quantitatively by three-dimensional micro-computed tomographic imaging (micro-CT) and to examine the activity of bone matrix production of osteoblasts and osteocytes during repair of alveolar bone defects, with *in situ* hybridization of the major bone matrix protein, type I collagen.

## Materials and methods

### *Animals*

Twelve-week-old male Wistar rats weighing from 250 to 280 g were used. They were obtained from the SLC

Correspondence: Yasuyuki Sasano, DDS, PhD, Division of Craniofacial Development and Regeneration, Tohoku University Graduate School of Dentistry, Sendai 980-8575, Japan. Tel: +81 22 717 8285, Fax: +81 22 717 8288, E-mail: sasano@anat.dent.tohoku.ac.jp
Received 18 November 2008; revised 26 January 2009; accepted 1 February 2009

Corporation (Kotoh, Shizuoka, Japan) and kept under a standard light–dark schedule and constant relative humidity. Stock diet and tap water were available *ad libitum*. All procedures were approved by the Animal Research Committee of Tohoku University.

*Surgical procedures and tissue preparation*

We divided 117 rats into two experimental groups. In one group, a standardized buccal (B) defect was made around the right first mandibular molar as a small defect, and in the second group, a standardized mesiobuccal (MB) defect was made as a large defect, also around the right first mandibular molar. In both groups, the left side served as a sham-operated control.

The rats were anesthetized with intraperitoneal sodium pentobarbital (4.5 mg 100 $g^{-1}$ of body weight) supplemented by ether inhalation. The surgical defect was created by preparing a 2 cm skin incision at the lower border of the mandible bilaterally (Zhao *et al*, 2004). The superficial fascia was separated, exposing the underlying masseter muscle, its ligamentary attachment to bone was severed at the inferior base of the defect, and both masseter and periosteum were separated from bone to expose the mandible. The oral mucosa on the superior wall of the surgically created access chamber was identified, and its attachment to the intraoral keratinized gingival margin was confirmed. The bone overlying the right mandibular first molar was removed with a round bar (Number 14, Bayer, Osaka, Japan) at low speed under saline irrigation (Park *et al*, 2007). The mesial roots, centro-buccal roots and distral roots of the first molar were carefully denuded of their periodontal ligaments, overlying cementum and superficial dentin, and the wounds were debrided with saline. The width of the B defect was defined as between the mesial edge of the mesial root and the distal edge of the distal root. The MB defect was between the mesio-lingual edge of the mesial root and the distal edge of the distal root. The floor of the defect was determined by the position of the root apex: the depth of the defect was determined as the point when bleeding from the periodontal ligament was observed on the exposed root surface (King *et al*, 1997). The overlying masseter over the exposed mandible was replaced, and the external incision was closed by surgical strings. The rats were fed a soft diet for 7 days after surgery.

Immediately after operation (week 0) or in weeks 3, 6, 12 or 24, the rats were anesthetized with sodium pentobarbital (5 mg 100 $g^{-1}$) supplemented by ether inhalation, and perfused through the aorta with 4% paraformaldehyde in 0.1 M phosphate buffer, pH 7.4 for micro-CT analysis, or 4% paraformaldehyde with 0.5% glutaraldehyde in 0.1 M phosphate buffer, pH 7.4 for *in situ* hybridization. The mandibles were resected and kept in the same fixative overnight at 4°C.

The mandibles for *in situ* hybridization were decalcified in autoclaved 10% EDTA in 0.01 M phosphate buffer, pH 7.4, for 4–8 weeks at 4°C. After dehydration through a graded series of ethanol solutions, the tissues were embedded in paraffin. Serial sections 5-$\mu$m thick were cut, and sections were processed for *in situ* hybridization or hematoxylin–eosin staining.

*Micro-computed tomography analysis*

For quantitative three-dimensional (3D) analysis of the alveolar bone defect, mandibles of 15 rats were scanned dorsoventrally using a microfocus X-ray CT system (SMX-225CT, Shimadzu, Kyoto, Japan) in weeks 0, 3, 6, 12 and 24. Three rats were fixed and examined for M defects and MB defects, respectively, at each time point. The sagittal plane of the specimens was set parallel to the X-ray beam axis. The specimens were scanned at a resolution of 80 $\mu$m in all three spatial dimensions. The scans were Gaussian filtered and segmented using a multilevel global thresholding procedure for the segmentation of enamel, dentin, and bone (Wilensky *et al*, 2005).

We used Voxblast software (Solution Systems, Tokyo, Japan) for imaging and analysis. The volume

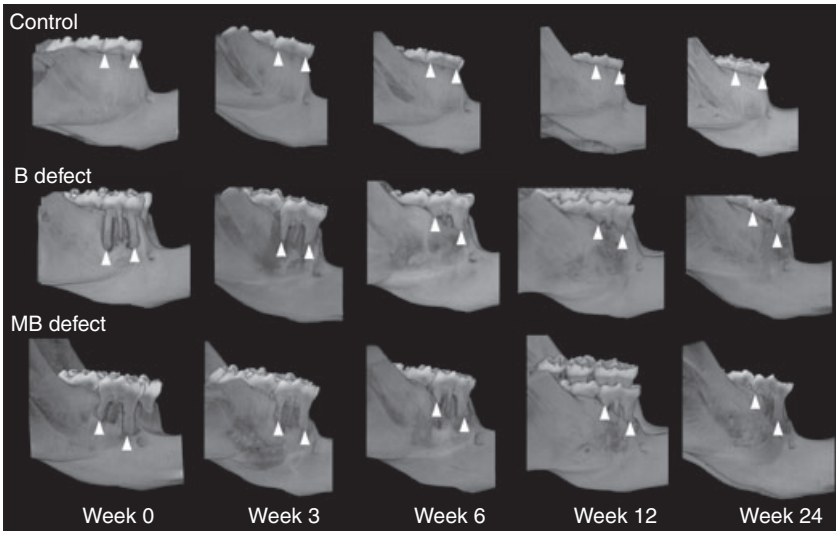


**Figure 1** Micro-CT image of the healing process in the rat alveolar bone defects. The crests of alveolar bone that are adjacent to mesial and distal roots of the mandibular first molar are indicated by arrowheads

of interest (VOI) was drawn with a slice-based method starting from the first slice containing the crown of the first molar and moving dorsally for 130 slices in the area between the mesial side of the mental foramen and the mesial side of the second molar. On the original 3D image, microstructural indices were calculated directly from the binarized VOI (Mavropoulos *et al*, 2004). The VOI of the bone between the mesial mental foramen and the mesial side of the second molar was measured.

*Statistical analysis*

All statistical analyzes were performed with Statcel statistical package (Statcel 2; OMS Inc., Tokorozawa, Japan). Data were analyzed by one-way analysis of variance (ANOVA), and then differences among mean values were analyzed using Tukey–Kramer multiple comparison tests. $P$ values $<0.05$ were considered significant. All the results were presented as mean values $\pm$ standard errors of the mean.

In situ *hybridization*

The protocol has been reported elsewhere (Nakamura *et al*, 2005) and is briefly described as follows:

The sections were deparaffinized and washed in phosphate-buffered saline (PBS), pH 7.4, and then immersed in 0.2 N HCl for 20 min. After being washed in PBS, the sections were incubated in proteinase K (20 g $ml^{-1}$; Roche, Mannheim, Germany) in PBS for 30 min at 37°C. After washing, the sections were dipped in 100% ethanol, dried in air and incubated with the antisense probe or the sense control probe (400 ng $ml^{-1}$) in a hybridization mixture for 16 h at 45°C. Digoxigenin-labeled, single-strand riboprobes for rat pro-alpha 1(I) collagen (Sasano *et al*, 2002) were used.

The sections were washed and treated with RNase (Type 1a, 20 $\mu$g $ml^{-1}$; Sigma, St Louis, MO, USA) for 30 min at 37°C. After washing, the hybridized probes were detected immunologically by using the Nucleic Acid Detection Kit (Roche), counterstained with methyl green, and mounted with a mounting medium.

At least two sections from each of three specimens at each stage were examined by using the same probe. The intensity of hybridization signals was evaluated by observing at least three fields of every section.

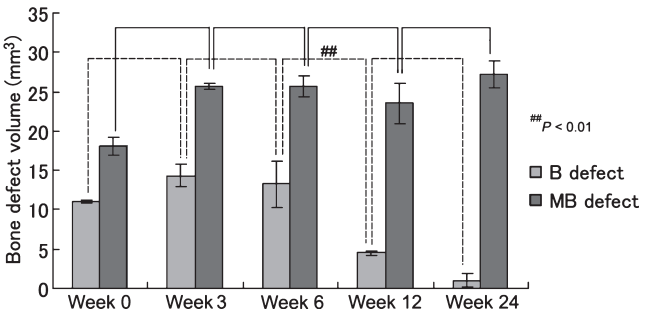


**Figure 3** Volume of bone defects from three-dimensional micro-CT analysis. The volume of B defects decreases by 88.3% to week 24, whereas the volume of MB defects shows little change

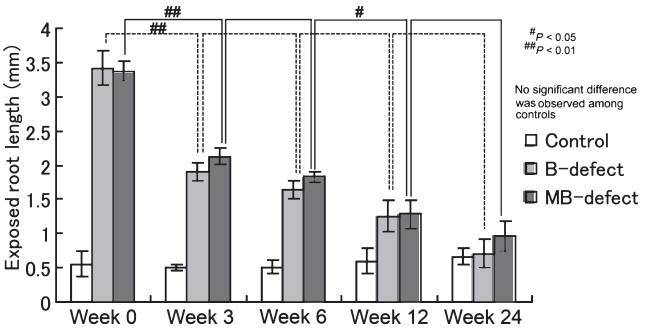


**Figure 4** Length of exposed distal roots from three-dimensional micro-CT analysis. The exposed root length decreases with time to week 3 in B defects and week 12 in MB defects. The length of the exposed distal root in week 24 in B defects is 20.8 % and in MB defects is 28.6 % of the length in week 0

## Results

The bone healing process in the alveolar bone defects is shown in Figure 1. Buccal (B) defects were repaired in week 24 significantly, whereas mesiobuccal (MB) defects were left largely unrepaired.

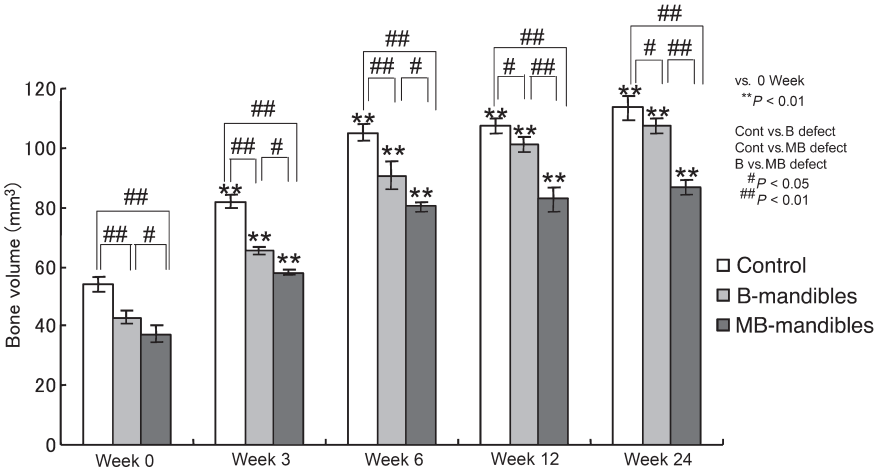


**Figure 2** Bone volume from three-dimensional micro-CT analysis. The volume of interest in the area between the mesial side of the mental foramen and the mesial side of the second molar of the mandible increases after the day of surgery for B mandibles and MB mandibles as well as control mandibles. Little increase in the volume is identified between weeks 6 and 24 in MB mandibles and control mandibles, and between weeks 12 and 24 in B mandibles. The volume of the control is significantly larger than that of B mandibles or MB mandibles to week 24, whereas the volume of B mandibles is significantly larger than that in MB mandibles

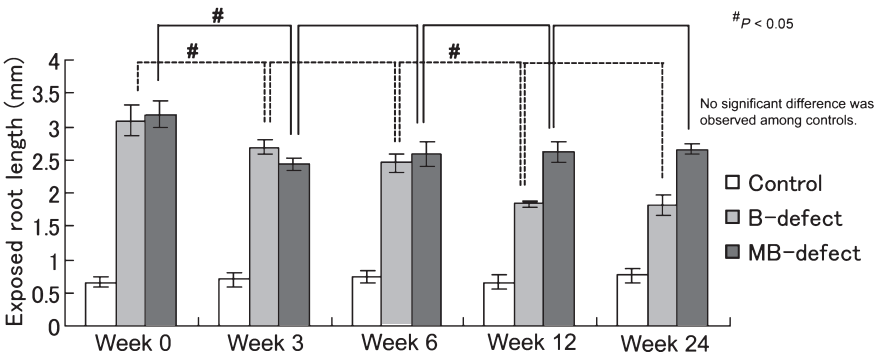


**Figure 5** Length of exposed mesial roots from three-dimensional micro-CT analysis. The exposed root length decreases with time to week 3 in MB defects and week 12 in B defects. The length of the exposed mesial root in week 24 in B defects is 58.9 % and in MB defects is 83.7 % of the length in week 0

*Bone volume of interest*

The bone VOI in the area between the mesial side of the mental foramen and the mesial side of the second molar of the mandible increased after the day of surgery for mandibles with B defects (B-mandibles) and MB defects (MB-mandibles) as well as control mandibles. The volume increased very little between weeks 6 and 24 in MB mandibles and control mandibles, and between weeks 12 and 24 in B mandibles. The volume of the control was significantly larger than that of B mandibles or MB mandibles to week 24, and the volume of B mandibles was significantly larger than that of MB mandibles (Figure 2).

The mean bone VOI ($\pm$s.e.m.) in the control mandibles in week 0 was 54.05 $\pm$ 0.84 $mm^3$ ($n$ = 3). The variation in the bone volume in B and MB mandibles

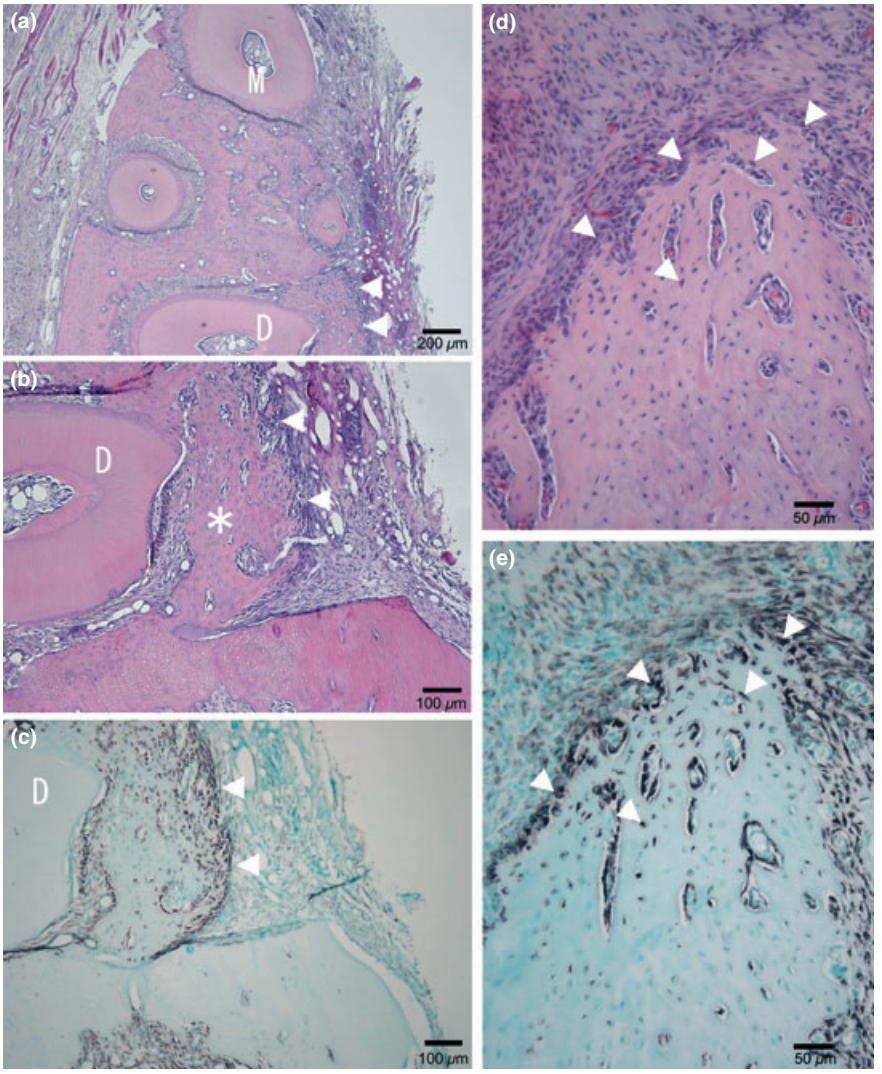


**Figure 6** Histology (**a**, **b**, **d**) and *in situ* hybridization(**c**, **e**) of MB defects in week 3. Inflammatory cell infiltration was not observed in week 3. New bone is formed more around distal roots than around mesial roots (**a**, **b**). Osteoblasts and osteocytes expressed type I collagen intensely in newly formed bone (**c**, **e**). M: mesial root, D: distal root, asterisk: new bone, arrowheads: osteoblasts and/or osteocytes

was small in week 0 (means 42.80 ± 1.25 $mm^3$ [$n = 3$] for B mandibles and 36.16 ± 1.50 $mm^3$ [$n = 3$] for MB mandibles).

*Bone defect volume*

The volume of the defects was calculated by subtracting the bone VOI in B mandibles or MB mandibles from that of their corresponding controls (Figure 3). The volume of B defects decreased significantly by 88.3% to week 24, whereas the volume of MB defects showed little change at week 24.

*Length of exposed roots*

The process of alveolar bone healing was evaluated by analyzing the length of the exposed roots, which was represented by the length from the cemento-enamel junction to the crest of the alveolar bone, adjacent to the mesial and distal roots, respectively (Misch *et al*, 2006). The length of the exposed distal root decreased significantly with time to week 3 in B defects and week 12 in MB defects (Figure 4). By contrast, the length of the exposed mesial root decreased significantly to week 3 in MB defects and week 12 in B defects (Figure 5). In week 24, the exposed distal root length in B defects was 20.8 % and in MB defects was 28.6 % of the length in week 0, whereas the exposed mesial root length in B defects was 58.9% and in MB defects was 83.7% of the length in week 0.

*Histology and in situ hybridization*

The healing process of alveolar bone in both B and MB defects was identical in regard to histology and *in situ* hybridization for type I collagen. Common features of both defects were described below, and representative data of MB defects was shown in figures.

Inflammatory cell infiltration was not observed in week 3. New bone was formed more around distal roots than around mesial roots (Figure 6a,b,d). Osteoblasts and osteocytes expressed type I collagen intensely in newly formed bone. (Figure 6c,e).

The bone defect was almost repaired around distal roots by week 6 (Figure7a). The boundary between newly formed bone and preexisting bone was identifiable (Figure 7b). Periodontal connective tissue intervened between cementum and newly formed alveolar bone. Bone defect repair was less around mesial roots (Figure 7a). Expression of type I collagen in newly formed bone was weaker (Figure 7c) than that in week 3.

The boundary between newly formed bone and preexisting bone around distal roots was no longer identifiable in weeks 12 (Figure 8a) and 24. Bone defect repair was less around the mesial root than around the distal root. Expression of type I collagen in osteoblasts and osteocytes was less intense and less extensive (Figure 8c) than that in week 3.

The denuded dentin and cementum were not repaired by week 12. By contrast, periodontal ligaments were

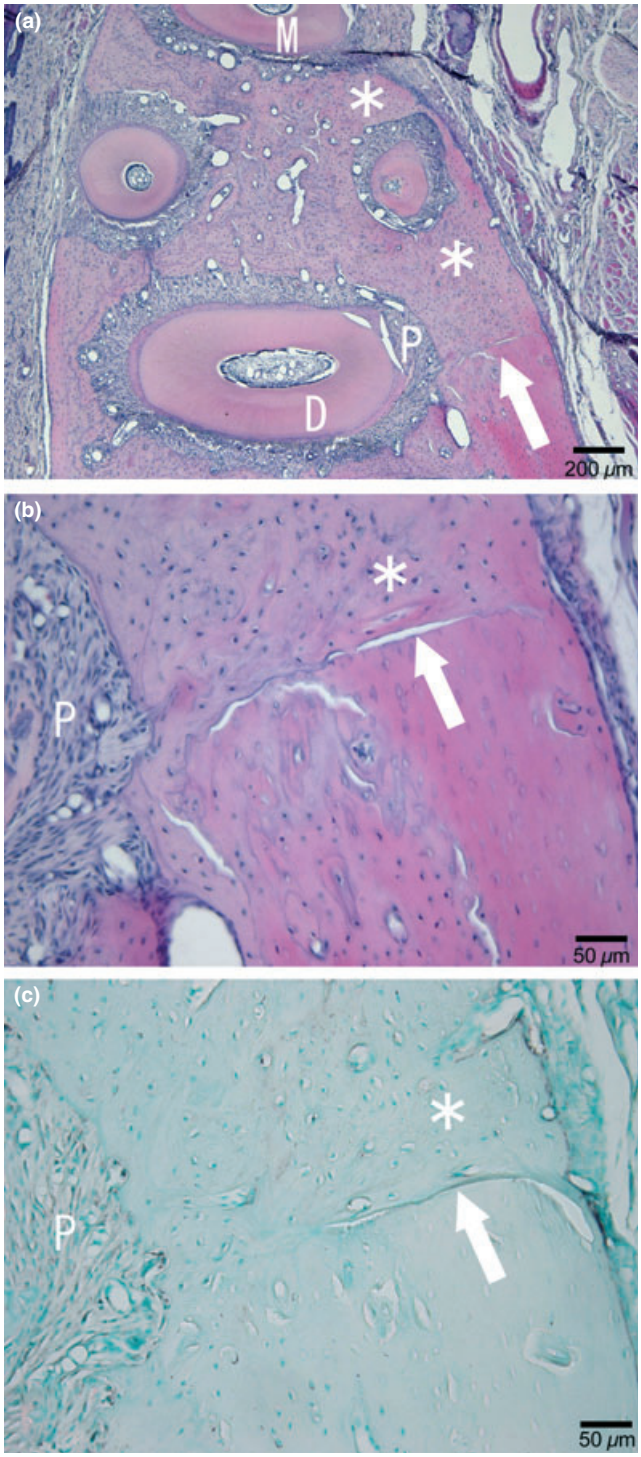


**Figure 7** Histology (**a**, **b**) and *in situ* hybridization (**c**) of MB defects in week 6. The bone defect is almost repaired around distal roots in week 6 (**a**, **b**). The boundary between new bone and preexisting bone is identifiable (**b**). Periodontal connective tissues intervene between cementum and newly formed alveolar bone. Bone defect repair is less around mesial roots (**a**). Expression of type I collagen in newly formed bone is weaker than that in week 3 (**c**). M: mesial root, D: distal root, P: periodontal connective tissues, asterisk: new bone, arrows: the boundary between new bone and preexisting bone

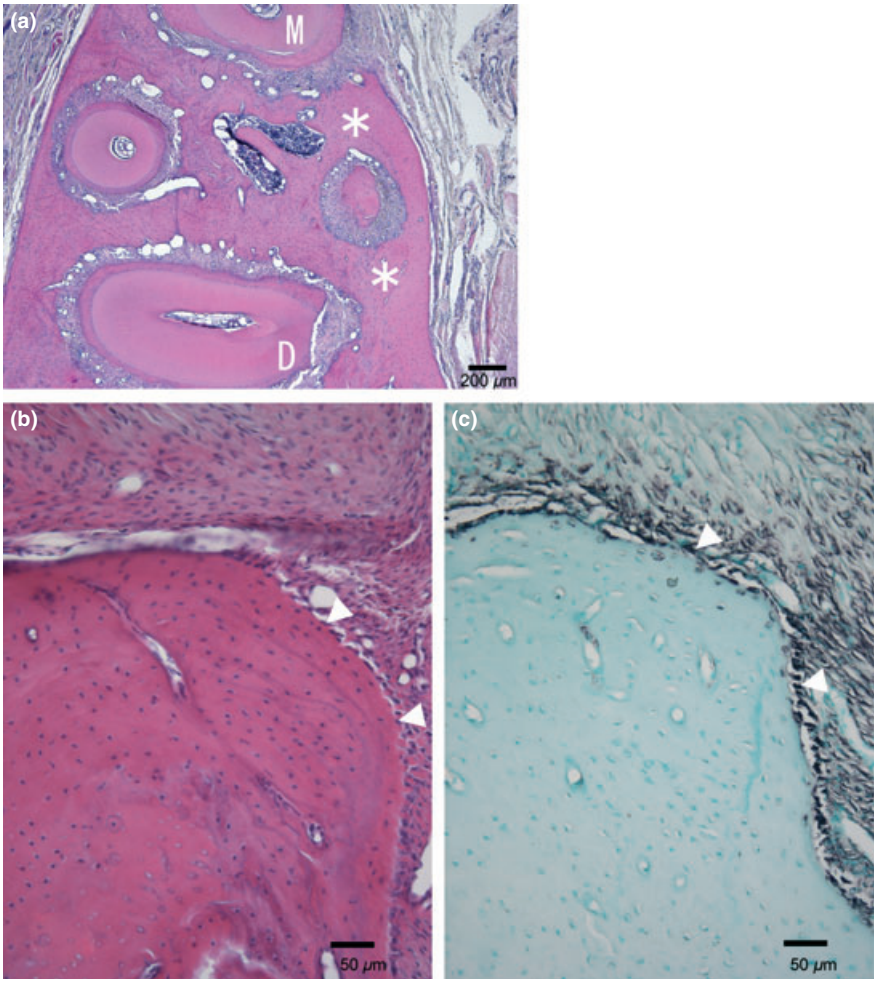


**Figure 8** Histology (**a**, **b**) and *in situ* hybridization (**c**) of MB defects in week 12. The boundary between newly formed bone and preexisting bone around distal roots is no longer identifiable in weeks 12 (**a**) and 24. Bone defect repair is less around the mesial root than around the distal root. Expression of type I collagen in ostoblasts and osteocytes is less intense and less extensive than that in week 3. M: mesial root, D: distal root, asterisk: new bone, arrowheads: osteoblasts and/or osteocytes

reorganized and periodontal ligament cells expressed type I collagen intensely in week 12 (Figure 9).

## Discussion

The 3D micro-CT analysis showed little variation in the bone VOI among control mandibles in week 0, which indicates that bone volume in control mandibles was uniform, with little individual variation. Also, the study showed little increase in bone volume between weeks 6 and 24 in control mandibles, while it increased in the first 6 weeks, which suggests that growth of the rat mandible reaches a peak at 18 weeks after birth, and keeps constant afterwards.

The variation in the bone volume among B mandibles and among MB mandibles was small in week 0. This suggests that the volume of both B defects and MB defects was constant, confirming that the experimental model is consistent and standardized.

The volume of B defects decreased to week 24. By contrast, the volume of MB defects showed little difference. The volume of the B defects had decreased or repaired in week 24 by 88.3%, while the volume of the MB defect in week 24 was comparable to that in week 0. This suggests that the B defect was almost repaired in 24 weeks, but the MB defect was not repaired. Therefore, the MB defect in the alveolar bone can be considered equivalent to the critical-size defect of the calvarial bone that is not ultimately repaired with bone (Honma *et al,* 2008).

The length of the exposed distal root in week 24 was reduced by 79.2 % in B defects and 71.4 % in MB defects from week 0, which means alveolar bone was repaired by 79.2% in B defects and by 71.4% in MB defects. By contrast, the length of the exposed mesial root in week 24 was reduced by 41.1 % in B defects and 16.3 % in MB defects, i.e. alveolar bone was repaired by 41.1% in B defects and by 16.3% in MB defects. New bone was formed more around distal roots than around mesial roots. This suggests that alveolar bone healing on the distal side proceeds better in both B and MB defects than that on the mesial side. Further investigation is required to clarify why alveolar bone heals better on the distal side.

Our previous studies showed that mRNA expression of type I collagen, the most abundant bone matrix protein, indicates the activity of matrix production in osteoblasts and osteocytes during bone healing as well as that of osteocalcin, the bone specific protein (Honma

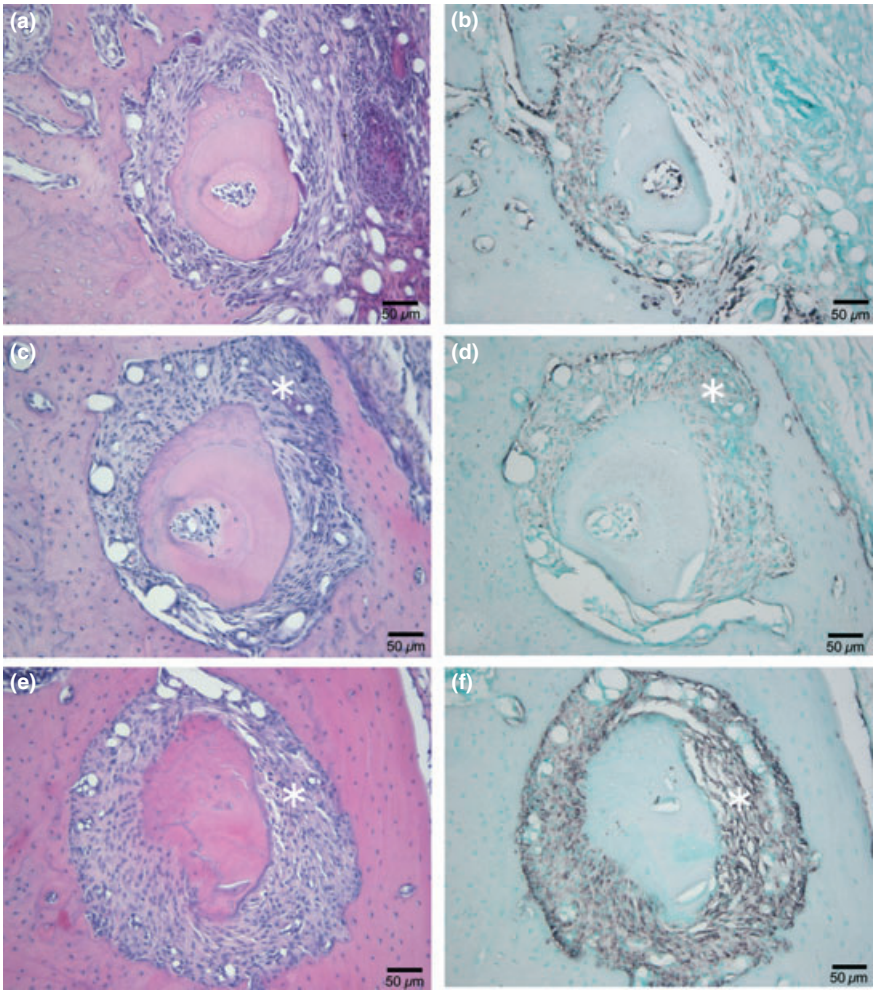


**Figure 9** Histology (**a**, **c**, **e**) and *in situ* hybridization for type I collagen (**b**, **d**, **f**) around centro-buccal roots of MB defects in weeks 3 (**a**, **b**), 6 (**c**,**d**) and 12 (**e**, **f**). Periodontal ligaments are reorganized and periodontal ligament cells express type I collagen intensely in week 12. Asterisk: periodontal ligaments

*et al*, 2008; Itagaki *et al*, 2008). Alveolar bone healing in this study may decline in week 6, as osteoblasts and osteocytes showed fewer signals of type I collagen compared to those in week 3. The 3D micro-CT analysis demonstrated that the MB defect is hardly repaired in week 6. Low expression of type I collagen by osteoblasts and osteocytes in the unrepaired MB defect in week 6 and thereafter suggests that the MB defect is not ultimately repaired with bone produced by osteoblasts and osteocytes, which indicates that the MB defect in the alveolar bone is a critical-size defect, on the basis of the data from the 3D micro-CT imaging analysis.

The data from histology and *in situ* hybridization showed that periodontal ligaments are reorganized, and periodontal ligament cells express type I collagen, whereas denuded cementum and dentin in the defect are not repaired. It is not known from where the periodontal ligament cells originated. They may have come from progenitors that resided in periodontal connective tissues around the defect and become differentiated to express type I collagen in week 12. Alternatively, periodontal ligament cells in intact periodontal ligaments surrounding the defect may have migrated to the defect region.

The study established for the first time a critical-size defect model of rat alveolar bone. Also, we have shown that the 3D micro-CT is a powerful tool for quantitatively analyzing healing of the complex morphology of alveolar bone. Further investigation using the experimental model and 3D micro-CT may provide a better understanding for clinical application of regenerative agents to treat alveolar bone loss.

## Acknowledgements

This work was supported in part by grants-in-aid (20592134, 20390527, 20300165) from the Ministry of Education, Science, Sports and Culture of Japan and Highly Functional Interface Science: Innovation of Biomaterials with Highly Functional Interface to Host and Parasite, Research and Education Funding for Inter-University Research Project, MEXT, Japan (Tohoku University Graduate School of Dentistry, Tohoku University Institute for Materials Research and Kyushu University Research Institute for Applied Mechanics). We wish to thank Dr. Megumi Nakamura, Division of Craniofacial Development and Regeneration, Tohoku University Graduate School of Dentistry, for her advice on this study. We also thank Mr. Yasuto Mikami and Mr. Masami Eguchi, Division of Craniofacial Development and Regeneration, Tohoku University Graduate School of Dentistry, for their technical assistance.

## Author contributions

H Ebina primarily performed the experiment. J Hatakeyama and M Onodera helped Ebina with tissue preparation and micro-CT analysis. T Honma and S Kamakura helped Ebina with surgical procedures and *in situ* hybridization. H Shimauchi edited the manuscript. Y Sasano, the corresponding author, desgined the research and analyzed the data.

## References

Cowan CM, Shi YY, Aalami OO *et al* (2004). Adisose-derived adult stromal cells heal critical-size mouse calvarial defects. *Nat Biotechnol* **22:** 560–567.

Cowan CM, Soo C, Ting K, Wu B (2005). Evolving concepts in bone tissue engineering. *Curr Top Dev Biol* **66:** 239–285.

Fritz ME, Jeffcoat MK, Reddy M *et al* (2000). Guided bone regeneration of large mandibular defects in a primate model. *J Periodontol* **71:** 1484–1491.

Honma T, Itagaki T, Nakamura M *et al* (2008). Bone formation in rat calvaria ceases within a limited period regardless of completion of defect repair. *Oral Dis* **14:** 457–464.

Itagaki T, Honma T, Takahashi I, Echigo S, Sasano Y (2008). Quantitative analysis and localization of mRNA transcripts of type I collagen, osteocalcin, MMP 2, MMP 8 and MMP 13 during bone healing in a rat calvarial experimental defect model. *Anat Rec* **291:** 1038–1046.

Kamakura S, Sasano Y, Homma H, Suzuki O, Kagayama M, Motegi K (1999). Implantation of octacalcium phosphate(OCP) in rat skull defects enhances bone repair. *J Dent Res* **78:** 1682–1687.

Kamakura S, Nakajo S, Suzuki O, Sasano Y (2004). New scaffold for recombinant human bone morphogenetic protein-2. *J Biomed Mater Res* **71A:** 299–307.

Kamakura S, Sasaki K, Honda Y, Anada T, Suzuki O (2006). Octacalcium phosphate combined with collagen orthotopically enhances bone regeneration. *J Biomed Mater Res B* **79:** 210–217.

King GN, King N, Cruchley AT, Wozney JM, Hughes FJ (1997). Recombinant human bone morphogenetic protein-2 promotes wound healing in rat periodontal fenestration defects. *J Dent Res* **76:** 1460–1470.

Lutolf MP, Weber FE, Schmoekel HG *et al* (2003). Repair of bone defects using synthetic mimetics of collagenous extracellular matrices. *Nat Biotechnol* **21:** 513–518.

Mavropoulos A, Kiliaridis S, Bresin A, Ammann P (2004). Effect of different masticatory functional and mechanical demands on the structural adaptation of the mandibular alveolar bone in young growing rats. *Bone* **35:** 191–197.

Misch KA, Yi ES, Sarment DP (2006). Accuracy of cone beam computed tomography for periodontal defect measurements. *J Periodontol* **77:** 1261–1266.

Nakamura M, Sone S, Takahashi I, Mizoguchi I, Echigo S, Sasano Y (2005). Expression of versican and ADAMTS1,4, and 5 during bone development in the rat mandible and hind limb. *J Histochem Cytochem* **53:** 1553–1562.

Park CH, Abramson ZR, Taba M Jr *et al* (2007). Three-dimensional micro-computed tomographic imaging of alveolar bone in experimental bone loss or repair. *J Periodontol* **78:** 273–281.

Sasano Y, Zhu JX, Tsubota M *et al* (2002). Gene expression of MMP8 and MMP13 during embryonic development of bone and cartilage in the rat mandible and hind limb. *J Histochem Cytochem* **50:** 325–332.

Wikesjö UME, Lim WH, Thomson RC, Cook AD, Wozney JM, Hardwick WR (2003). Periodontal repair in dogs: evaluation of a bioabsorbable space-providing macroporous membrane with recombinant human bone morphogenetic protein-2. *J Periodontol* **74:** 635–647.

Wilensky A, Gabet Y, Yumoto H, Houri-Haddad Y, Shapira L (2005). Three-dimensional quantification of alveolar bone loss in *Porphyromonas gingivalis*-infected mice using micro-computed tomography. *J Periodontol* **76:** 1282–1286.

Zhao M, Jin Q, Berry JE, Nociti FH Jr, Giannobile WV, Somerman MJ (2004). Cementoblast delivery for periodontal tissue engineering. *J Periodontol* **75:** 154–161.